Electronic Supplementary Material (ESI) for Analytical Methods.

A highly effective peroxidase mimic nanozyme of S, N-Carbon dots decorated Cerium organic framework based colorimetric detection of Hg^{2+} ion and thiophanate methyl

Rajakumari Jesuraj [a] , Panneerselvam Perumal [a]*

[a] Department of Chemistry, SRM Institute of Science and Technology, Kattankulathur, 603 203, Tamil Nadu, India.

* Corresponding Author-Dr. Panneerselvam Perumal- Department of Chemistry, SRM Institute of Science and Technology, Kattankulathur, 603 203, Tamil Nadu, India; E-mail: panneerp1@srmist.edu.in; panneerchem82@gmail.com; Phone: +91 9688538842; ORCID: https://orcid.org/0000-0003-2647-6835.

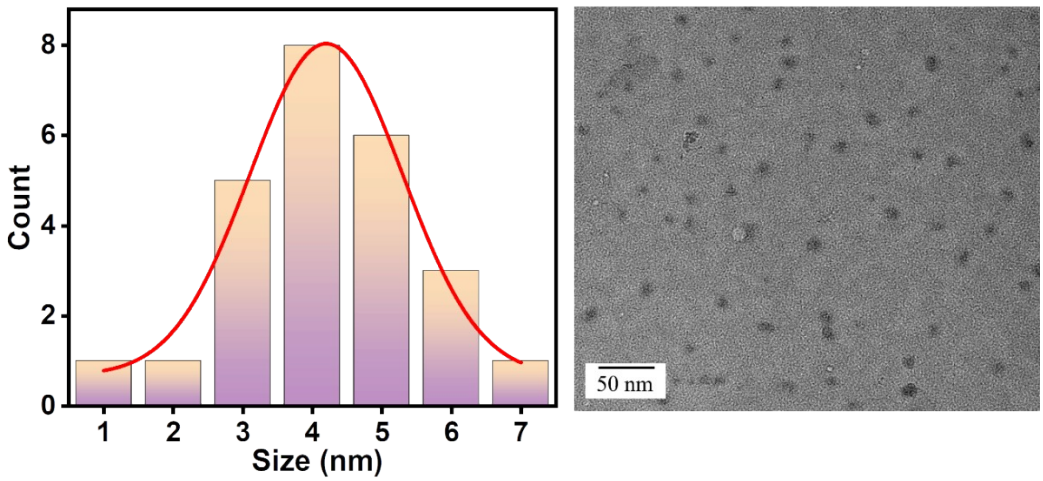

Figure S1. Particle size distribution histogram for S, N-CDs

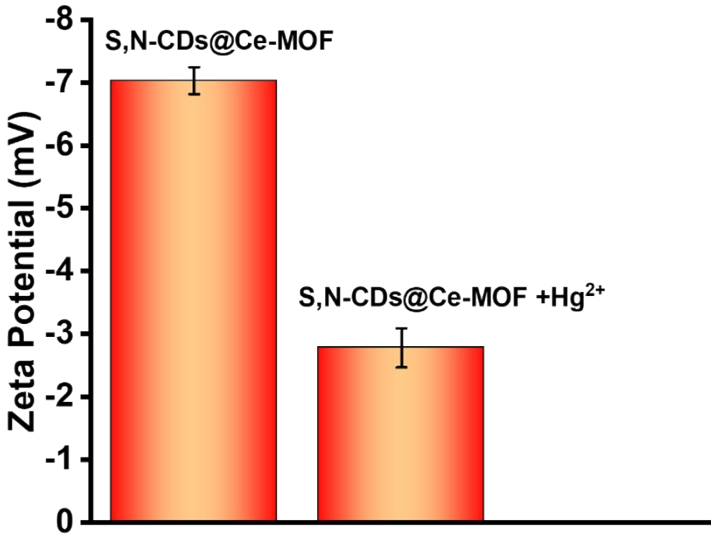

Figure S2 Zeta analysis before and after the addition of Hg^{2+}

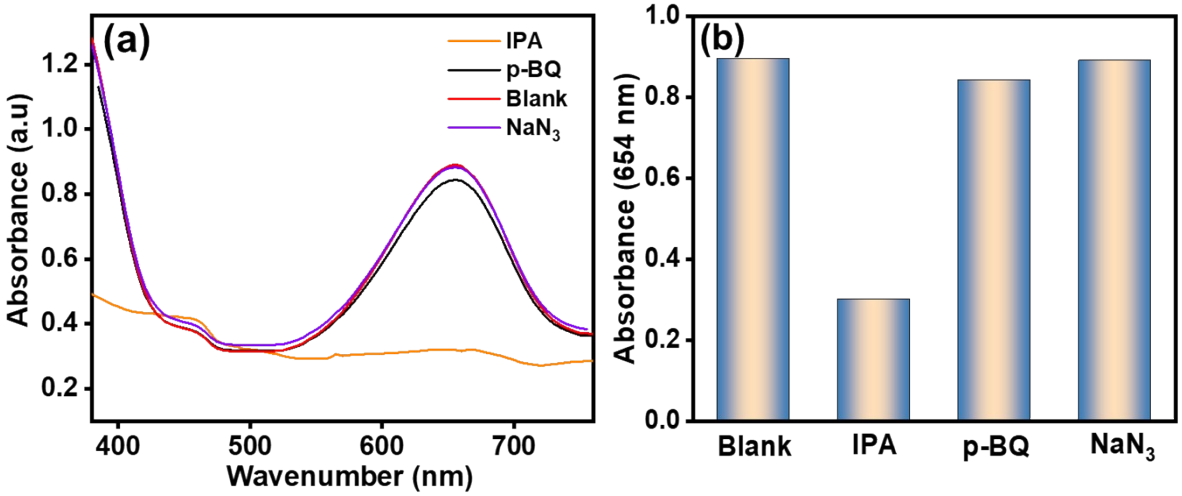

Figure S3. Radical confirmation analysis

We looked at a selectivity analysis for Hg^{2+} and TM with sugar, ions, and amino acids (**Figure S4 a-b**). However, sugars, ions, and amino acids do not interfere with the detection of Hg^{2+}. Meanwhile, in TM detection amino acids have a minor interference but it takes double the time and quantity needed compared to the detection of TM so it's negligible. However, minor interference also prohibited by using a NEM masking agent.

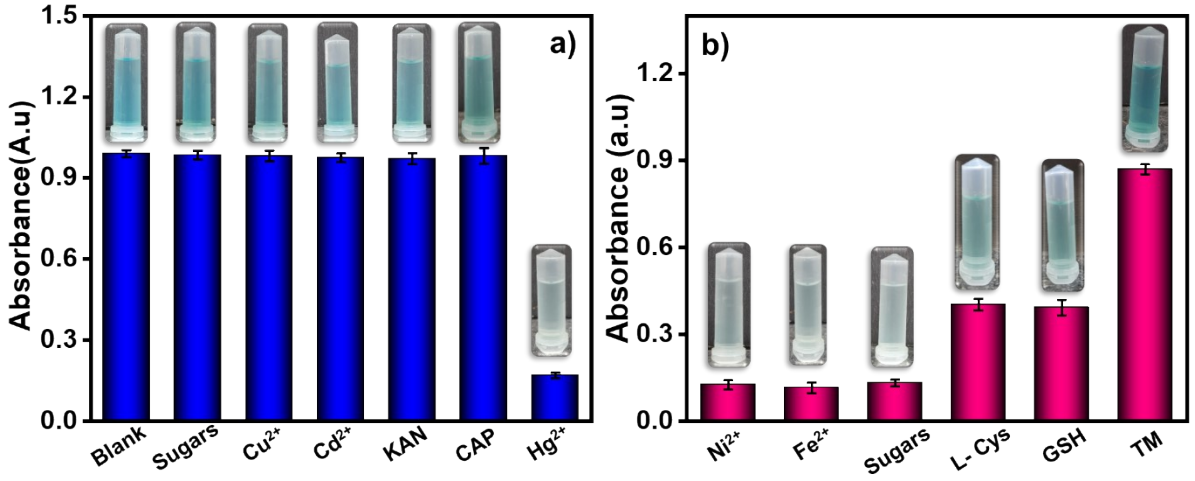

Figure S4. (a-b) Selectivity analysis for Hg^{2+} and TM with sugars, ions, and amino acids respectively.

Kinetic analysis of S, N-CDs@Ce-MOF Nanozyme

Using a steady-state kinetics, the peroxidase-like catalytic performance of S, N-CDs@Ce-MOF with TMB and H_2O_2 as substrates. In brief, the experiment was carried out by varying the concentration of H_2O_2 from 0.5 to 5 mM while TMB at 2 mM as fixed concentration and repeating the experiment by varying the concentration of TMB from 0.5 to 4 mM while H_2O_2 at 3 mM concentration. In addition, the Michaelis-Menten curves and Lineweaver–Burk plots for H_2O_2 and TMB are shown in **FigS5**. S, N-CDs@Ce-MOF nanozyme's Michaelis-Menten constant (Km) and maximal reaction velocity (Vmax), were calculated using the Lineweaver–Burk double reciprocal equation (1).

$$\frac{1}{V} = \frac{K_m}{V_{max}} \frac{1}{[S]} + \frac{1}{V_{max}} \qquad (1)$$

Where V_{max} is the maximal reaction velocity, V is the initial velocity, and [S] is the substrate concentration, K_m is the Michaelis constant. In this case, the enzyme's catalytic activity is shown by the V_{max} value, while the K_m value indicates the affinity of the enzyme to the substrate. The K_m value of S, N-CDs@Ce-MOF using H_2O_2 and TMB were 0.828mM and 1.145 mM respectively. The V_{max} values of the S, N-CDs@Ce-MOF with H_2O_2 and TMB

substrates were 2.50 (10^{-8} Ms^{-1}) and 5.17 (10^{-8} Ms^{-1}) respectively. **Table S1** provides the K_m value and the V_{max} value of the S, N-CDs@Ce-MOF with comparison to other nanozymes. As a result, S, N-CDs@Ce-MOF have a good binding affinity towards H2O2 and TMB which enhanced the catalytic activity.

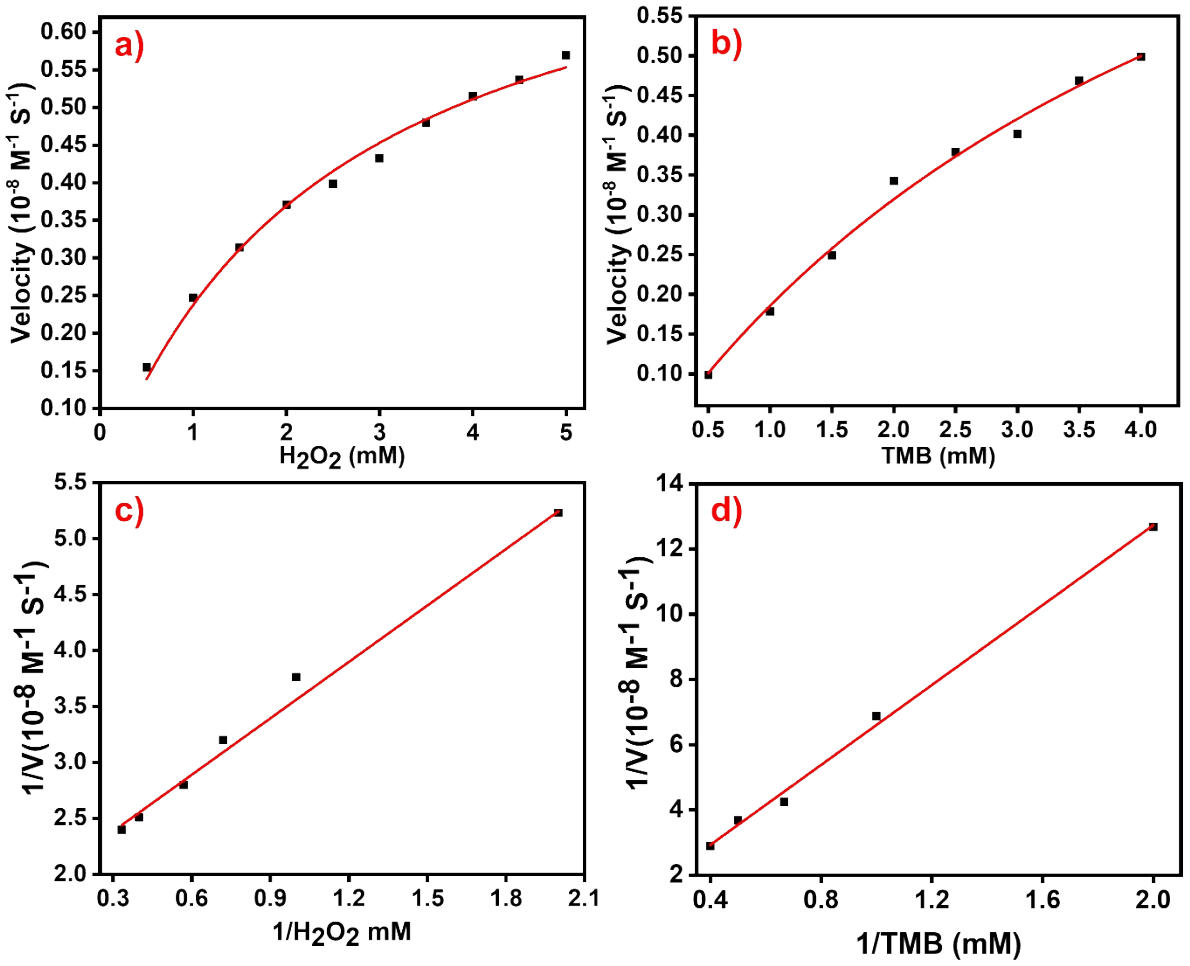

Figure S5. Steady-state kinetic assay of S, N-CDs@Ce-MOF by using (a and b) Michaelis-Menten curve for H_2O_2 and TMB and (c and d) Lineweaver–Burk plots of the double reciprocal of the Michaelis– Menten equations for H_2O_2 and TMB respectively.

Table S1. Comparison of K_m and V_{max} with other previously reported literature

Catalyst	Substrate	K_m (mM)	V_{max}	Reference
HRP	TMB	0.434	10.0 (10^{-8} Ms^{-1})	[1]
	H_2O_2	3.702	8.71 (10^{-8} Ms^{-1})	
N, S-CDs	TMB	0.387	0.167 (10^{-8} Ms^{-1})	[2]
	H_2O_2	0.106	0.530(10^{-8} Ms^{-1})	
Fe/CeO2 HBs	TMB	0.52	8.84 (10^{-8} Ms^{-1})	[3]
	H_2O_2	0.36	5.83 (10^{-8} Ms^{-1})	
S, N-CDs@Ce-MOF	TMB	1.145	5.17 (10^{-8} Ms^{-1})	This work
	H_2O_2	0.828	2.50 (10^{-8} Ms^{-1})	

In addition, we quantitatively measured the specific activity of S, N-CDs@Ce-MOF by measuring the absorbance intensity shown in **Figure S6.** The nanozyme activity (units) was calculated by the following equation,

$$b_{nanozyme} = \frac{V}{(\in X\, l)} X \left(\frac{\Delta A}{\Delta t}\right)$$

Where $b_{nanozyme}$is the nanozyme catalytic activity expressed in units, V is the total volume of the reaction (μL); l is the path length of light traveling in the cuvette (cm); $\in$ is the colorimetric substrate molar absorbance coefficient (TMB = 39,000 M^{-1} cm^{-1}) ΔA/Δt represents the rate of change at absorbance 654nm min^{-1}.The specific activity of the nanozyme calculated by

$$a_{nanozyme} = b_{nanozyme}/[m]$$

Where, $a_{nanozyme}$ is specific activity which is expressed in units per milligram (U mg^{-1}), m is the mass of the nanozyme in mg[4]

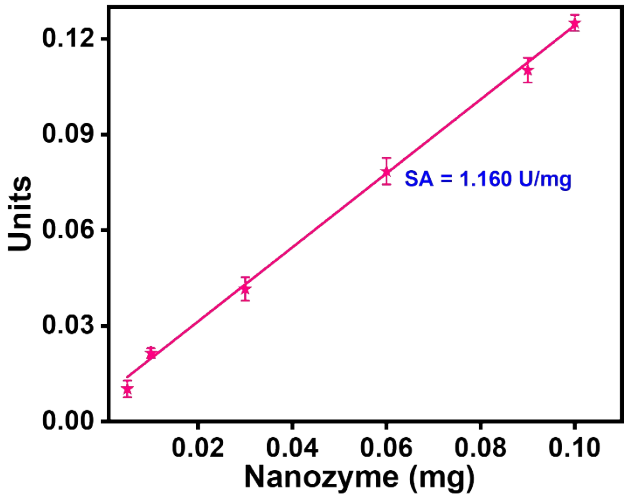

Figure S6. Specific activity of S, N-CDs@Ce-MOF

Table S2. Comparison of the proposed Hg^{2+} sensor with other reported methods

Sensing Method	Sensing Probe	Linear Range	LOD	Reference
Colorimetric	ED-AgNPs	0-120 µM	70 nM	[5]
Colorimetric	Gin-AgNPs	0-160 µM	1.46 µM	[6]
Colorimetric	Fe_3O_4@C@AuNPs	0.001-25 µM	0.0435 µM	[7]
Fluorescent	FA@Ag-Pt QDs	2-20 µm	40 nM	[8]
Colorimetric	S, N-CDs@Ce-MOF	0-0.20 µM	0.01 µM	This work

Table S3. Comparison of the proposed thiophanate methyl sensor with other reported methods

Sensing Method	Sensing Probe	Linear Range	LOD	Reference
Colorimetric	Cit-AgNPs	2-100 µM	0.12 µM	[9]
Fluorescent	Cu-CDs	0.00-0.65 µM	0.78 µM	[10]
Colorimetric	Cu@NC	0.2-15 µg mL^{-1}	0.11 µM	[11]

Colorimetric	S, N-CDs@Ce-MOF	0.03-0.20 μM1	0.03 μM	This work

1 J.-W. Zhang, H.-T. Zhang, Z.-Y. Du, X. Wang, S.-H. Yu and H.-L. Jiang, *Chemical Communications*, 2014, **50**, 1092–1094.

2 V. K. Singh, P. K. Yadav, S. Chandra, D. Bano, M. Talat and S. H. Hasan, *J Mater Chem B*, 2018, **6**, 5256–5268.

3 L. Chen, X. Zhu, J. Tang, X. Ouyang, Y. Liao, Y. Lu, J. Wang, Z. Wei, B. Xi and L. Tang, *ACS ES&T Water*, 2023, **3**, 2318–2327.

4 B. Jiang, D. Duan, L. Gao, M. Zhou, K. Fan, Y. Tang, J. Xi, Y. Bi, Z. Tong, G. F. Gao, N. Xie, A. Tang, G. Nie, M. Liang and X. Yan, *Nat Protoc*, 2018, **13**, 1506–1520.

5 A. Jabbar, A. Abbas, N. Assad, M. Naeem-ul-Hassan, H. A. Alhazmi, A. Najmi, K. Zoghebi, M. Al Bratty, A. Hanbashi and H. M. A. Amin, *RSC Adv*, 2023, **13**, 28666–28675.

6 K. Plaeyao, R. Kampangta, Y. Korkokklang, C. Talodthaisong, A. Saenchoopa, S. Thammawithan, K. Latpala, R. Patramanon, N. Kayunkid and S. Kulchat, *RSC Adv*, 2023, **13**, 19789–19802.

7 B. Motlhaedi, J. Mokone and M. T. Alula, *Inorg Chem Commun*, 2023, **156**, 111296.

8 Y. Tang, W. Gou, X. Lv, X. Zhou, J. Hao, C. Sun, T. Sun, L. Hu and Z. Yan, *Food Chem*, 2023, **408**, 135259.

9 M. Zheng, Y. Wang, C. Wang, W. Wei, S. Ma, X. Sun and J. He, *Spectrochim Acta A Mol Biomol Spectrosc*, 2018, **198**, 315–321.

10 X. Yue, C. Zhu, R. Gu, J. Hu, Y. Xu, S. Ye and J. Zhu, *Foods*, , DOI:10.3390/foods11213336.

11 M. Zhang, Y. Wang, N. Li, D. Zhu and F. Li, *Biosens Bioelectron*, 2023, **237**, 115554.